IEEE Copyright Statement:

Miniaturized Force-Indentation Depth Sensor for Tissue Abnormality Identification during Laparoscopic Surgery

Hongbin Liu, Jichun Li, Qi-ian Poon, Lakmal D. Seneviratne and Kaspar Althoefer

Abstract—**This paper presents a novel miniaturized force-indentation depth (FID) sensor designed to conduct indentation on soft tissue during minimally invasive surgery. It can intra-operatively aid the surgeon to rapidly identify the tissue abnormalities within the tissue. The FID sensor can measure the indentation depth of a semi-spherical indenter and the tissue reaction force simultaneously. It make use of with fiber optical fiber sensing method measure indentation depth and force and is small enough to fit through a standard trocar port with a diameter of 11 mm.**

The created FID sensor was calibrated and tested on silicone block simulating soft tissue. The results show that the sensor can measure the indentation depth accurately and also the orientation of the sensor with respect to the tissue surface whilst performing indentation.

.

I. Introduction

There have been notable advances in robotic-assisted minimally invasive surgery (MIS) or laparoscopic surgery in recent years. The most well known robotic surgical systems includes the Zeus^{TM} Surgical System from Computer Motion [1](Computer Motion was merged with Intuitive Surgical in 2003) and the da Vinci^{TM} Surgical System (Intuitive Surgical, Inc.[2]). Distinct advantages of these robotic systems include high distal dexterity, enhanced 3D vision, motion scaling and tremor filtering as well as direct hand-eye coordination eliminating reversed tool motions. These advances result in improved ergonomics and also allow complex surgical procedures, which are usually difficult to be conducted by conventional minimally invasive means such as coronary artery bypass grafting [3] and mitral valve repair[4] to be effectively performed. However, the lack of haptic feedback in current robot-aided minimally invasive surgery systems is still one of the major downsides of such systems.

Manuscript received September 15, 2009.

H. Liu is with the Department of Mechanical Engineering, Kings College London, UK (e-mail: hongbin.liu@kcl.ac.uk).

J. Li is with the Department of Mechanical Engineering, Kings College London, UK (e-mail: jichun.li@kcl.ac.uk).

K. Althoefer is with the Mechanical Engineering Department, King's College London, Strand, London, WC2R 2LS, UK (e-mail: k.althoefer@kcl.ac.uk).

L. D. Seneviratne is with the Mechanical Engineering Department, King's College London, Strand, London, WC2R 2LS, UK (e-mail: lakmal.seneviratne@kcl.ac.uk).

The research leading to these results has been partially supported by the HANDLE project, which has received funding from the European Communitity's Seventh Framework Programme (FP7/2007-2013) under grant agreement ICT 231640

The authors have shown in the past [5] [6] that rolling indentation employing a force-sensitive wheel is feasible to obtain reaction force information from a large tissue area in short time. The approach proves to be capable of identifying the location of tumors within soft tissue and is feasible to compensate the loss of haptic sensation associated with the robotics-assisted MIS. Indenting a soft tissue with a rolling probe at a constant indentation depth allows the continuous and rapid measurement of the tissue stiffness as rolling takes place. The abnormalities within soft tissue can be readily identified through examination of the stiffness distribution as tissue abnormalities are often stiffer than the surrounding normal tissue. The major limitation of the above method is that the rolling indentation depth needs to be kept constant throughout the experiment. In our earlier work this was achieved by preregistering the tissue surface before experiments are conducted (i.e. creating a map of the tissue's height distribution). Preregistering a soft tissue surface is time consuming and if applied into MIS, the tissue shift during a surgery may induce inaccuracies to the surface registration. The aim of this paper is to introduce a novel force-indentation depth (FID) sensor which can measure the indentation depth of an indenter and the tissue reaction force concurrently during indentation.The FID sensor has been created using with a fiber optical sensing method for both indentation depth sensing and force sensing. The developed sensor prototype fits through a standard trocar port of 11mm in diameter. The use of non-electronics components allows the device enduring the clinical sterilization procedure and lays the foundation for MR-compatibility.

II. Literature Survey

The indentation depth of an indenter is given by the relative displacement of the tip of indenter with respect to the soft tissue surface. Hence the indentation depth can be measured by acquiring the local tissue deformation when the wheel rolls over the soft tissue. So far, a number of techniques have been developed to intra-operatively acquire the tissue deformation during a MIS.

Intra-operative three-dimensional computed tomography (CT) technique can provide information regarding soft tissue morphology and structure. This technique is particularly suitable for differentiating the bones from other tissues and thus has been often used in the image-guided surgery such as oral surgery [7], orthopedic surgery [8], neurosurgery [9] as well as the prostate brachytherapy[10] However, due to the cost and the radiation exposure associated with such techniques, they are not ideal for intraoperatively measuring the tissue deformation during a minimally invasive surgery.

A relatively inexpensive and practical technique to measure the tissue deformation is to use the stereo vision. The stereo vision utilizes two or more cameras to interpolate the three-dimensional (3D) information of a subject including the shape, texture and depth, based on computer vision techniques and the known geometry coordinates between the cameras [11]. Using a high speed camera, this technique can extract information in real time, and thus it can be used to recover the 3D structure of the operating field [12] and track the temporal motion of deformable tissue surfaces [13] during a minimally invasive surgery. While the applications of optical vision method in minimally invasive surgery are promising and progressing, one major downside with this technique is by the difficult in extracting features on curved and specular surfaces. In medical application, especially during a surgical procedure where the internal organs are all surrounded in fluids and have curved surfaces, the stereo vision method is not always effective [11].

To extract features on curved surfaces, the laser line scanner can be used. While this type of system provides high resolution 3D images, its speed is usually not real-time. Hence it is difficult to require feature information from moving objects using such a system. A more practical way to obtain the 3D information of a curved object in real time is the structured light technique.[11],[14],[15] This technique utilizes a projector to project a known light pattern onto an object. The light pattern on the object is then viewed from a camera mounted next to the projector. Given the known position and orientation of both camera and projector, the information including the shape and the distance of object can be calculated. However to use such a technique to infer the real time wheel indentation depth is problematic. First, while this technique works effectively for a curved object, it has difficulty in extracting information on specular surfaces which are often encountered in the internal body. Second, it is difficult to integrate the wheeled probe with the projector and the camera while maintaining the small size of the whole device.

In view of limitations associated with the above intra-operative 3D imaging techniques, a new technique to measure the indentation depth is proposed in this paper. Our method is to develop a fiber optic FID sensor to concurrently measure the wheel indentation depth and the tissue reaction force during the wheel-tissue interaction. The advantages of utilizing such a method are twofold: 1) the method is effective and low cost as it can accurately measure the wheel indentation depth in real-time without the need for high speed camera system and time consuming imaging processing techniques; 2) the FID sensor can be easily miniaturized and integrated with the force-torque sensor, still small enough to fit through a standard trocar port.

III. The Design of the Miniaturized FID Sensor

The miniaturized FID sensor consists of a fiber optical force sensor (FS) and four fiber optical displacement sensors (DS-1, DS-2, DS-3, and DS-4). Fig.1 and Fig.2 indicate the structures of the miniaturized FID sensor. The basic form of the optic sensing principle consists of a pair of transmitting fiber and receiving fiber as well as a reflector. The transmitting fiber carries the light generated from a light source and projects the light to the reflector. The reflector then reflects the light into the receiving fiber, and finally the intensity of reflected light is detected by an optical detector. Since the change of the displacement between the reflector and fiber tips (h) varies the reflected light intensity, the motion of reflector can be detected through the measuring the reflected light intensity [17]. The transmitting fiber and receiving fiber can be placed with an inclined angle φ to increase the sensitivity. It has been demonstrated in [17] [18] that, along the increase of the bent angle φ from 0^o to 90^o, the sensing sensitivity increases and displacement sensing range decreases.

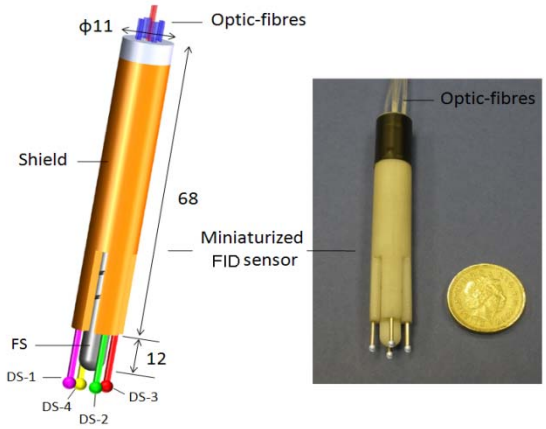

Fig.1. The miniaturized FID sensor consisting of one fiber optical fiber force sensor (FS) as well as four fiber optical fiber displacement sensors (DS), including DS-1, DS-2, DS-3 and DS-4; a coin of one pound sterling is used to indicate the size of the miniaturized FID sensor. All units are in "mm".

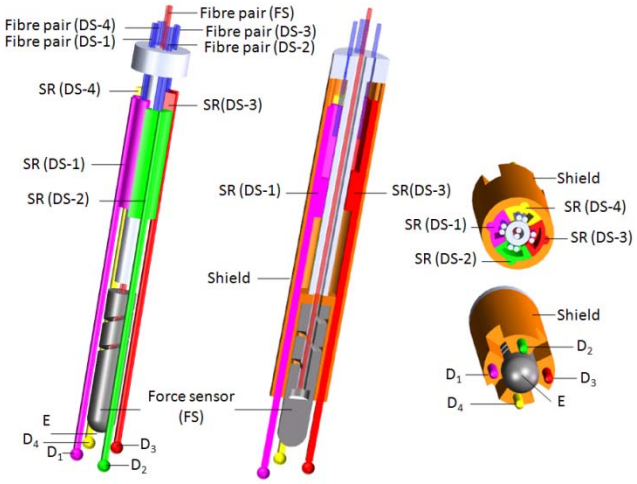

Fig.2 The structures of the miniaturized FID sensor; the main components of the device include a optic- fiber force sensor (FS), and four fiber optical fiber displacement sensors, DS-1, DS-2, DS-3 and DS-4, each consisting of a sliding rod (SR) attached to a reflector and a pair of transmitting fiber and receiving fiber. SR(DS-1), SR(DS-2), SR(DS-3) and SR(DS-4) represent the sliding rod of displacement sensor DS-1, DS-2, DS-3 and DS-4, respectively D_1, D_2, D_3 and D_4 indicate the contactors connecting with the displacement sensors; E indicates the indenter connecting with the FS.

. The fiber optical FS is composed of the semi-spherical indenter E, a helical-cut sensing structure attached with a

reflector and a fiber pair including a transmitting fiber and a receiving fiber, as shown in Fig.3(a). The helical-cut sensing structure behaviours like a spring with high elastic modulus; when an axial force is imparted, the helical-cut sensing structure is compressed, causing a the small movement of reflector towards the fiber tips. By measuring the displacement of the reflector, the applied axial force can be interpreted. The transmitting fiber and receiving fiber are used to detect the distance between the fiber tip and the reflector. The tips of both transmitting fiber and the receiving fiber are bent with an angle of 15^o and placed towards each other to increase the sensitivity of the FS, Fig. 3 (a) (inclined angle φ= 30^o). The shield prevents the shape of helical-cut sensing structure being altered by lateral forces.

The four displacement sensors, DS-1, DS-2, DS-3 and DS-4, are arranged in an equal space inside the shield. SR(DS-1), SR(DS-2), SR(DS-3) and SR(DS-4) represent the sliding rod of displacement sensor DS-1, DS-2, DS-3 and DS-4, respectively. Four semi-spherical contactors, D_1, D_2, D_3 and D_4, connect with the sliding rods of the four displacement sensor. The shield guides each sliding rod to move freely along its axial direction. Each displacement sensor consists of a sliding rod attached with a reflector and a pair of transmitting and receiving fibers, Fig.3 (b). The transmitting fiber and receiving fiber are used to detect the distance between the fiber tip and the reflector. The two fibers are arranged in parallel with no bent angles to increase the sensing range of the displacement sensor.

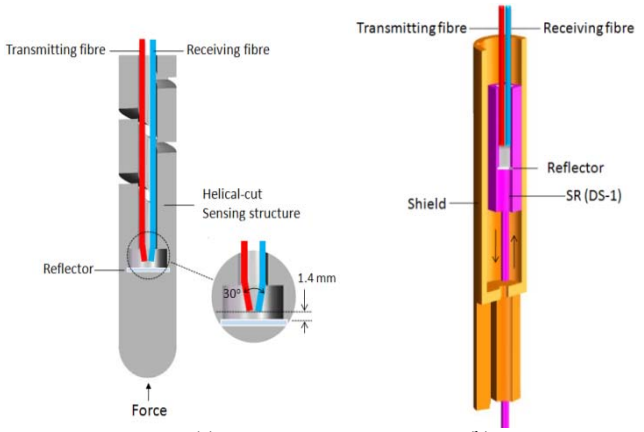

Fig.3. Schematics of the fiber optical force sensor (a) and the displacement sensor (b); in both sensors, a pair of transmitting fiber and receiving fiber is used to measure the distance between the fiber tip and the reflector. In the force sensor, the reflector is attached to a helical-cut sensing structure; in the displacement sensor, the reflector is attached to a sliding rod which has free movement axially.

Five high intensity LEDs are used for generating transmitting light, the change of light intensity for DSs and FS are measured using photo detectors, the received signals are amplified using the Op-Amp AD620 which has ultra-low input current noise. The optic circuit is placed inside metal box to reduce the signal noises. A 16-bit data acquisition card (NI PCI 6013) and the LabView^{TM} 8.0 software package are used to acquire the measured signals. The sampling rate is 100 Hz.

IV. Measuring the Indentation Depth and the Sensor Orientation

During a indentation conducted using the miniaturized FID sensor, the fiber optical FS measures the forces acting on the indenter E while the four semi-spherical contactors (D_1, D_2, D_3 and D_4) slide over the tissue surrounding the indenter. When the indenter indents into the tissue surface the contactors are free to slide axially and therefore remain on the surface of the tissue. Due to soft tissue's high local deformability, the indentation contour raises from the indentation point to the surface following an exponential curve. Therefore, by measuring the distance between the deepest indentation point and the positions of the contactors, the indentation depth of the indenter and the orientation of the indenter with respect to the tissue surface can be established.

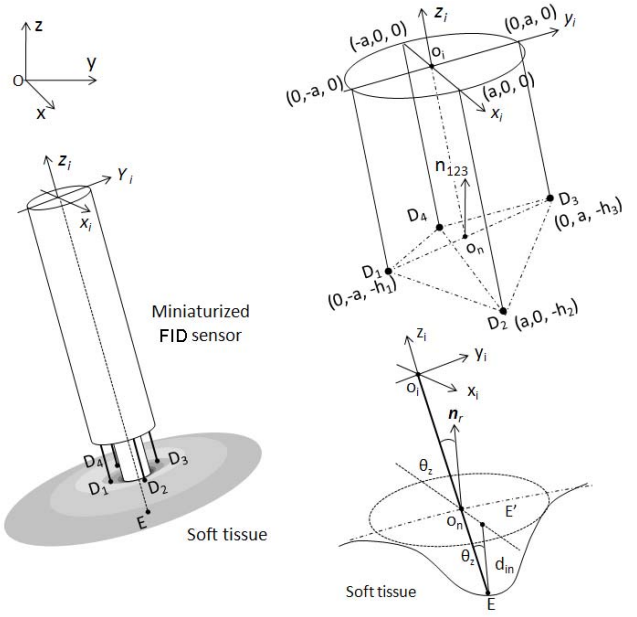

Fig .4. Acquisition of the indentation depth and the orientation of the indenter with respect to the tissue surface during indentation using the miniaturized FID sensor; positions of contactors, D_1 D_2, D_3 and D_4 are (0, -a, -h_1), (a, 0, -h_2), (0, a, -h_3) and (-a, 0, -h_3) respectively in the coordinate system (x_i, y_i, z_i),where a is the radius of the miniaturized FID sensor (a = 5.5 mm), h_1, h_2, h_3 and h_4 are the distances between the contactors and the x_i y_i –plane; o_n indicates the average position of the four contactors.

It is defined the (x, y, z) to be the globe Cartesian coordinate system. The coordinate system (x_i , y_i , z_i) is attached to the miniaturized FID sensor as indicated in Fig.4 (z_i is align with the central axis of the sensor). When the sensor indents into the soft tissue, the four contactors can configure four planes, $D_1D_2D_3$, $D_2D_3D_4$, $D_1D_2D_4$ and $D_1D_3D_4$. The normal direction of the contacted tissue surface can be approximated by averaging the normal vectors of the planes $D_1D_2D_3$, $D_2D_3D_4$, $D_1D_2D_4$ and $D_1D_3D_4$.

As seen in Fig. 4, defining the n_{123} to be the unit vector normal to the plane $D_1D_2D_3$, the n_{123} can be calculated as:

$$n_{123} = \frac{D_2D_3 \times D_1D_2}{|D_2D_3 \times D_1D_2|}.$$

Defining the positions of contactors, D_1 D_2, D_3 and D_4 to be (0, -a, -h_1), (a, 0, -h_2), (0, a, -h_3) and (-a, 0, -h_3) respectively in the coordinate system (x_i, y_i, z_i),where a is the radius of the miniaturized FID sensor (a = 5.5 mm), h_1, h_2, h_3 and h_4 are the distances between the corresponding contactors and the x_i y_i -plane, the vector D_2D_3 and D_2D_1 can be calculated as:

$D_2D_3 = o_iD_3 - o_iD_2 = -ai + aj + (h_2-h_3)k,$
$D_2D_1 = o_iD_1 - o_iD_2 = -ai - aj + (h_2-h_1)k,$

Thus

$$D_2D_3 \times D_1D_2 = \begin{vmatrix} i & j & k \\ -a & a & h_2-h_3 \\ -a & -a & h_2-h_1 \end{vmatrix}$$

$= a(2h_2-h_1-h_3)i - a(h_1-h_3)\,j - 2a^2k,$

where i, j and k are the unit vectors along x_i axis, y_i axis and z_i axis, respectively. Hence

$$n_{123} = \frac{a(2h_2-h_1-h_3)}{r_{123}}i + \frac{a(h_3-h_1)}{r_{123}}j + \frac{2a^2}{r_{123}}k,$$

where r_{123} is the norm of the vector n_{123},

$$r_{123} = \sqrt{a^2(2h_2-h_1-h_3)^2 + a^2(h_3-h_1)^2 + 4a^4}.$$

Following the above procedures, the unit vector n_{124} which is normal to plane $D_1D_2D_4$ can be calculated as:

$$n_{124} = \frac{a(h_2-h_4)}{r_{124}}i + \frac{a(h_2+h_4-2h_1)}{r_{124}}j + \frac{2a^2}{r_{124}}k,$$

where r_{124} is the norm of the vector n_{124},

$$r_{124} = \sqrt{a^2(h_2-h_4)^2 + a^2(h_2+h_4-2h_1)^2 + 4a^4};$$

the unit vector n_{134} which is normal to plane $D_1D_3D_4$ is

$$n_{134} = \frac{a(h_1+h_3-2h_4)}{r_{134}}i + \frac{a(h_3-h_1)}{r_{134}}j + \frac{2a^2}{r_{134}}k$$

where r_{134} is the norm of the vector n_{134},

$$r_{134} = \sqrt{a^2(h_1+h_3-2h_4)^2 + a^2(h_3-h_1)^2 + 4a^4};$$

the unit vector n_{234} which is normal to plane $D_2D_3D_4$ is

$$n_{234} = \frac{a(h_2-h_4)}{r_{234}}i + \frac{a(2h_3-h_2-h_4)}{r_{234}}j + \frac{2a^2}{r_{234}}k,$$

where r_{234} is the norm of the vector n_{234},

$$r_{234} = \sqrt{a^2(h_2-h_4)^2 + a^2(2h_3-h_2-h_4)^2 + 4a^4}.$$

The normal vector to the contacted tissue surface, n_r, can be approximated by the resultant vector of n_{123}, n_{124}, n_{134}, and n_{234},

$$n_r = n_{123} + n_{124} + n_{134} + n_{234}.$$

The angle θ_z between the normal vector of the tissue surface and the z_i axis (central axis of the sensor) can be determined as:

$$cos\theta_z = 2a^2\left(\frac{1}{r_{123}} + \frac{1}{r_{124}} + \frac{1}{r_{134}} + \frac{1}{r_{234}}\right), \quad (1)$$

and the distance between the deepest indentation point and the positions of the contactors along the normal direction of contact, d_m is determined as:

$$d_m = cos\theta_z\left(h_e - \frac{h_1+h_2+h_3+h_4}{4}\right), \quad (2)$$

where r_{123}, r_{124}, r_{134} and r_{234} are the vector norms of n_{123}, n_{124}, n_{134}, and n_{234} , respectively, h_e is the distance between the tip of the indenter E and the x_i y_i -plane.

Since the helical-cut sensing structure of the fiber optical fiber FS has high elastic modulus, the change of distance h_e during indentation is reasonable to be neglected. Hence distance h_e can be considered as a constant value. Moreover, the distance h_1, h_2, h_3 and h_4 can be measured using the corresponding displacement sensors, DS-1, DS-2, DS-3 and DS-4. Thus the d_m and orientation of the indenter with respect to soft tissue surface can be detected using the miniaturized FID sensor. To obtain the indentation depth, d_{in}, the relationship between the d_m and d_{in} need to be calibrated on different tissue sample. The calibration can be then used to interpret the indentation depth d_{in} from measuring the d_m.

V. Calibration of the FID sensor

To calibrate the four displacement sensors and the force sensor of the FID sensor, the entire unit is attached to the distal tip of a Mitsubishi RV-6SL, a 6-DoF (degree of freedom) robotic manipulator, to allow for accurate motion control. Fig.5 shows the calibration setup using the FID sensor.

For the force sensor calibration, the fiber optic FS is compressed against an ATI Mini40 sensor. During the calibration, the fiber optic FS was slowly advanced towards and retrieved from the Mini40, varying the interaction force between the two sensors. The signals measured from the fiber optic FS and the corresponding force values measured from the Mini40 were recorded. The calibration results are shown in Fig.6. For the calibration of the four DSs, each sliding rod of DS was moved increasingly from its minimum length to the maximum length over a range of 16 mm. the displacement h_1, h_2, h_3 and h_4 and the corresponding signal from each sliding rod were recorded respectively. The calibration results are shown in Fig.7.

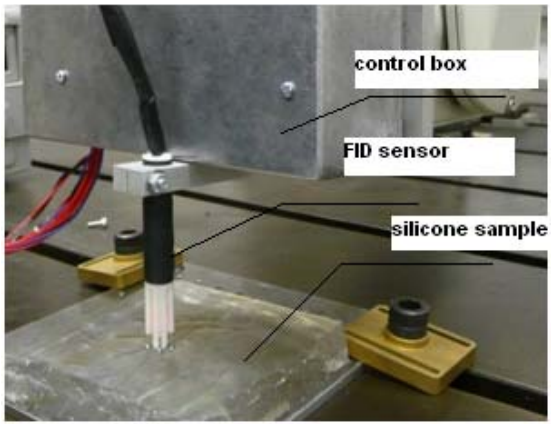

Fig.5. The calibration setup using the FID sensor, the robotic manipulator and a silicone sample

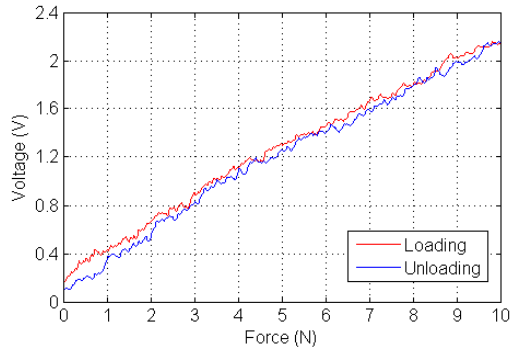

Fig.6. The calibration results of fiber optic force sensor

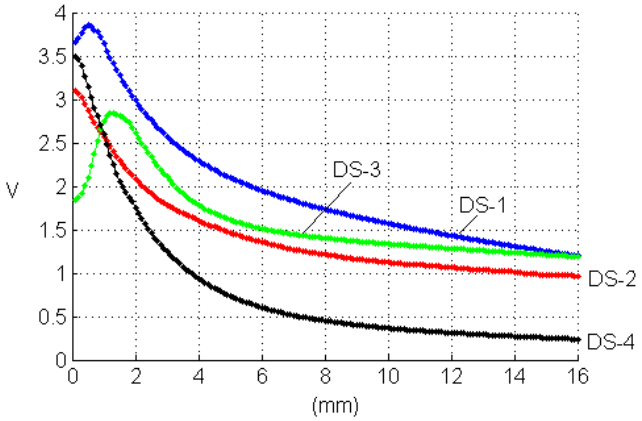

Fig.7. The calibration of fiber optic displacement sensors: the blue curve represent the measured voltage output of DS-1and corresponding distance between the contactor D_1 and the bottom surface of shield, the red curve is for DS-2 , the green curve is for DS-3, and the black color is for DS-4.

To calibrate the relationship between the indentation depth d_{in} and the distance d_m, a silicone block, with the dimension of 30 mm in height, 50 mm in width and 100 mm in length, was used. During the calibration, the FID sensor was vertically indented into the silicone sample at a speed of 0.1 mm/s until d_{in} reached 6 mm. The value of d_{in} and the corresponding d_m were recorded. The calibration results are shown in Fig.8. From the calibration, it was found that the relationship between the indentation depth d_{in} and the distance d_m can be expressed as

$$d_{in} = 0.44(e^{0.66d_m} - 1). \quad (3)$$

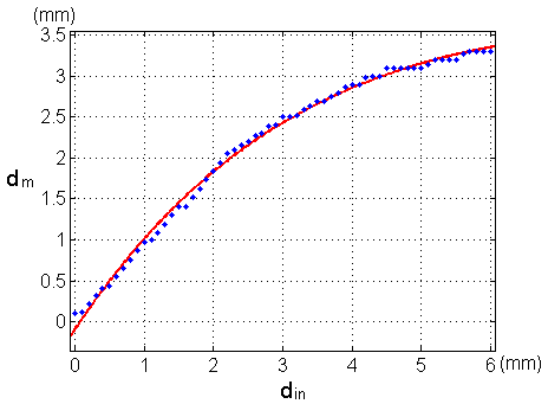

Fig.8. The calibration of relationship between the indentation depth d_{in} and the distance d_m.The blue dots are the measured values and the solid red line is the fited curve.

VI. Performance Analysis

In order to analysis the performance of the FID sensor, the robotic manipulator was used to drive the sensor to slide across the silicone sample along y axis by a distance of 40 mm at different angle θ_z (the angle between the normal vector of the tissue surface and the central axis of the sensor). There were four angle selected, θ_z = 0°, 5°, 10° and 15°. The indentation depth was linearly increased from from 0 mm to 6 mm while the angle θ_z was kept constant at 0°. Indentation depth increased linearly from 0 mm to 5 mm while the angle θ_z = 5°, 10° and 15°. During the experiments, the distance d_m was calculated using Eq.1, Eq.2 and then the indentation depth, d_{in} was determined from the d_m using Eq.3. Fig.9 shows the comparison between the measured indentation depth and ground truth data.

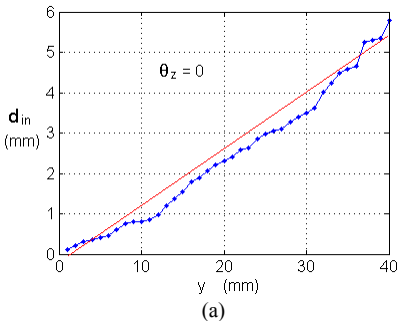

(a)

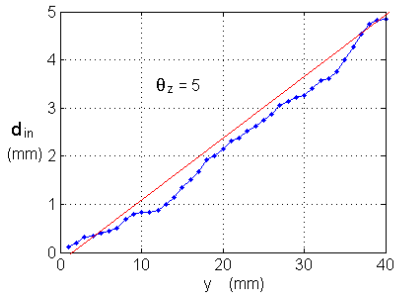

(b)

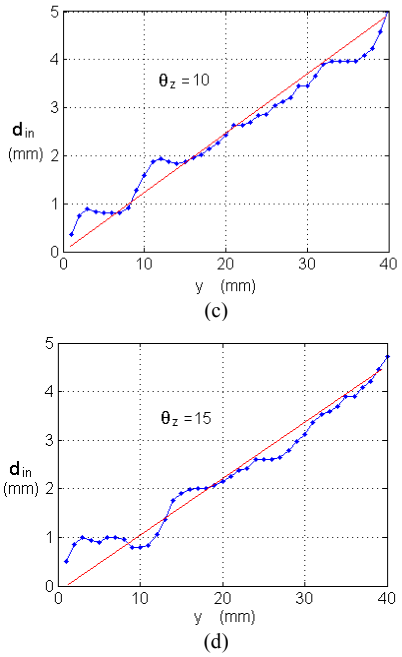

Fig.9. The comparison between the measured indentation depth (blue dots) and ground truth data (red solid line) with different angle θ_z including $\theta_z = 0^o$, 5^o, 10^o and 15^o, showing in (a), (b), (c), (d) respectively.

The error analysis showed that the RMSE for $\theta_z = 0^o$ is 0.256, the RMSE for $\theta_z = 5^o$ is 0.233, the RMSE for $\theta_z = 10^o$ is 0.276, the RMSE for $\theta_z = 15^o$ is 0.316. It can be seen that for each selected angle θ_z, the FID sensor can measure the indentation depth reasonably well.

VII. Conclusion

This paper describes a miniaturized FID sensor which fits through a standard trocar port with an inner diameter of 11 mm. The validation experiment conducted on a silicone sample demonstrates that the developed miniaturized FID sensor can accurately and concurrently measure both the indentation depth of the indenter and the tissue reaction force during tool-tissue interaction. Since the stiffness can be acquired using the tissue deformation and the corresponding tissue reaction force, it is expected that the stiffness distribution of the investigated soft tissue can be identified from by sliding the FID sensor over a large area of tissue without prior tissue surface registration. This indicates the feasibility of using the miniaturized FID sensor for tissue abnormalities identification during minimally invasive surgery. The proposed FID sensor has potential to aid surgeon in locating tumors during minimally invasive surgery.

It is noted that, although using a semi-spherical indenter instead of a rolling wheel simplified the manufacturing of the, the spherical indenter may cause large tangential (shear) force while sliding across tissue, potentially damaging the underlying tissue. Furthermore, the interaction dynamics between the fixed spherical indenter and soft tissue has not been investigated in this study. Thus further experimental study of interaction dynamics would be required for implementing the spherical indenter

It is also noted that at this stage of the research into indentation depth measuring, gravity is used to extend the measuring mechanism outward in order to guarantee contact between the contactor and the tissue. Future work will aim at studying other mechanisms in order to ensure that indentation depth can be measured independently of the direction of gravity, as it is needed if the tool is to be moved arbitrarily with regards to lines of gravity.

References

[1] Uranues, S., et al. "Early experience with telemanipulative abdominal and cardiac surgery with the ZeusTM Robotic System", Euro. Surg., Vol. 34, pp. 190-193,2002

[2] Guthart,G. S. and Salisbury, J. K.Jr. "The IntuitiveTM telesurgery system: Overview and application" Proc. IEEE Int. Conf. Robotics and Automation, pp. 618-621,2000.

[3] Tabaie, H. A., et al. "Endoscopic coronary artery bypass graft (ECABG) procedure with robotic assistance" ,The Heart Surgery Forum, Vol. 2, pp. 310-317, 1999.

[4] Murphy, D. A., et al. J. Thorac. Cardiovasc. Surg., Vol. 132, pp. 776-781, 2006.

[5] H. Liu, D. Noonan, L. Seneviratne, P. Dasgupta, K. Althoefer, Rolling Indentation for Tissue Abnormality Localization during Minimally Invasive Surgery, IEEE Trans. on Biomedical Eng., **57**(2). 2010 pp. 404 - 414.

[6] Liu, H., et al. "The Rolling Approach for Soft Tissue modeling and Mechanical Imaging during robot-assisted Minimally Invasive Surgery" ,Proc. IEEE Int. Conf. Robot. Autom. ,pp. 846-850, 2008.

[7] Pohlenz, P, et al. "Major mandibular surgical procedures as an indication for intraoperative imaging", J Oral Maxillofac Surg, Vol. 66, pp. 324-329, 2008

[8] Love, G. J., Pillai, A. and Gibson, S. "Use of the mini C-arm for wrist fractures--establishing a diagnostic reference level", Radiat Prot Dosimetry, Vol. 128, pp. 309-311,2008

[9] Moore, A. J. and Newell, D. W. "Neurosurgery: principles and practice" , Springer, pp. 123-138,2005.

[10] Jain, A, et al. " Intra-operative 3D guidance in prostate brachytherapy using a non-isocentric C-arm", Int Conf Med Image Comput Comput Assist Interv., Vol. 10(Pt 2), pp. 9-17,2007.

[11] Keller, K. and Ackerman, J. "Real-time Structured Light Depth Extraction", SPIE proceedings. pp. 11-18, 2000.

[12] Mourgues, F., Devernay, F. and Coste- Manière, E. "3D reconstruction of the operating field for image overlay in 3D-endoscopic surgery" ,Proceedings of International Symposium on Augmented Reality. pp. 191-192, 2001.

[13] Stoyanov, D, Darzi, A and Yang, G.Z. "A practical approach towards accurate dense 3D depth recovery for robotic laparoscopic surgery", Comput Aided Surg, Vol. 10, pp. 199-208, 2005.

[14] Hu, G. and Stockman, G. 4 "3-D surface solution using structured light and constraintpropagation", IEEE Transactions on Pattern Analysis and Machine Intelligence, Vol. 11, pp. 390-402, 1989.

[15] Lavoie, P., Ionescu, D. and Petriu, E.M. "3D object model recovery from 2D images using structured light", IEEE Transactions on Instrumentation and Measurement, Vol. 53, pp. 437- 443

[16] Puangmali, P., et al., Optical fiber sensor for soft tissue investigation during minimally invasive surgery. 2008. Proc. IEEE Int. Conf. Robot. Autom. pp. 2934-2939.

[17] Buchade, P.B. and Shaligram, A.D. Simulation and experimental studies of inclined two fiber displacement sensor. 2006, Sensors and Actuators A , Vol. 128, pp. 312–316.